Ain Shams Engineering Journal (2016) 7, 755–765

Ain Shams University

Ain Shams Engineering Journal

www.elsevier.com/locate/asej
www.sciencedirect.com

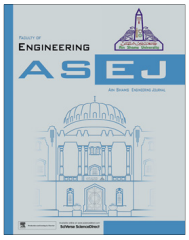

ENGINEERING PHYSICS AND MATHEMATICS

Double diffusive unsteady convective micropolar flow past a vertical porous plate moving through binary mixture using modified Boussinesq approximation

Isaac Lare Animasaun *

Department of Mathematical Sciences, Federal University of Technology, Akure, Ondo State, Nigeria

Received 6 February 2015; revised 25 April 2015; accepted 19 June 2015
Available online 28 August 2015

KEYWORDS

Constant vortex viscosity;
Micropolar fluid;
Modified Boussinesq approximation;
Thermophoresis;
Variable viscosity;
Vertical surface through binary mixture

Abstract The problem of unsteady convective with thermophoresis, chemical reaction and radiative heat transfer in a micropolar fluid flow past a vertical porous surface moving through binary mixture considering temperature dependent dynamic viscosity and constant vortex viscosity has been investigated theoretically. For proper and correct analysis of fluid flow along vertical surface with a temperature lesser than that of the free stream, Boussinesq approximation and temperature dependent viscosity model were modified and incorporated into the governing equations. The governing equations are converted to systems of ordinary differential equations by applying suitable similarity transformations and solved numerically using fourth-order Runge–Kutta method along with shooting technique. The results of the numerical solution are presented graphically and in tabular forms for different values of parameters. Velocity profile increases with temperature dependent variable fluid viscosity parameter. Increase of suction parameter corresponds to an increase in both temperature and concentration within the thin boundary layer.

1. Introduction

Non-Newtonian fluids are common fluids in industrial and engineering processes in which there is no linear relationship between stress and deformation rate as such fluid flows along horizontal or vertical surface. Within the past few years, the dynamic and behavior of non-Newtonian fluid have received considerable attention in the field of heat and mass transfer and thermal science owing to their great applications in the industrial production of molten polymers, pulps, fossils fuels and fluids containing certain additives. Immense contributions to the body of knowledge (i.e. toward the understanding of the dynamics of non-Newtonian fluids) can be found in Refs. [1–8]. Gebhart et al. [9] focused on the physics of a flow along vertical surface and explained extensively how fluid flows along vertical surface. In natural convection, fluid surrounding a

* Tel.: +234 8034117546.
E-mail address: anizakph2007@gmail.com.

Peer review under responsibility of Ain Shams University.

ELSEVIER Production and hosting by Elsevier

http://dx.doi.org/10.1016/j.asej.2015.06.010

Nomenclature

(x, y)	cartesian coordinates
t	time
T	temperature of the fluid
N	angular velocity
j	micro-inertia density
T_∞	dimensional free stream temperature
Q	activation enthalpy
E_A	activation energy
C_p	specific heat at constant pressure
R_G	universal gas constant
S_c	schmidt number
V_T	thermophoretic velocity
K_r	chemical reaction rate
$h(\eta)$	dimensionless microrotation
L_1	time dependent microrotation parameter
R_a	radiation number
G_r	modified thermal Grashof number
$f(\eta)$	velocity profile
(u, v)	velocity components along x, y directions respectively
g	acceleration due to gravity
C	concentration of the fluid
T_w	dimensional surface temperature
C_w	dimensional surface concentration
C_∞	dimensional free stream concentration
c	suction
h_q	heat generation parameter
U_o	uniform velocity at free stream
n	order of the chemical reaction
ΔH	enthalpy change
D_m	coefficient of mass diffusivity
R_A	arrhenius term
K_1	microrotation parameter
D_a	Damkholer number
G_c	modified solutal Grashof number
P_r	Prandtl number

Greek symbols

ξ	variable viscosity parameter
ϑ	kinematic viscosity
κ	thermal conductivity
τ	vortex viscosity
μ	dynamic viscosity
ω	activation energy
θ	dimensionless temperature
β	volumetric thermal-expansion coefficient
ψ	stream function
α	absorption coefficient
σ	Stefan–Boltzmann constant
ρ	fluid density
η	similarity variable
θ_w	dimensionless wall temperature
ϕ_w	dimensionless wall concentration
λ	thermophoretic parameter
ϕ	dimensionless concentration
β^*	volumetric solutal-expansion coefficient
γ^*	spin gradient viscosity

heat source receives heat energy; the fluid tends to becomes less dense and rises. The surrounding cooler fluid moves to replace it [9]. Bird et al. [10] reported that this cooler fluid is heated and the process continues forming convection current; this process transfers heat energy from the hot region to cool region. The driving force for free convective is buoyancy, a positive differences in fluid density. According to all the previous published articles on fluid flow along vertical surface, it is worth noticing that existence of buoyancy in the fluid domain is incorporated into the momentum equation based on the fact that wall temperature is greater than free stream temperature and the temperature decreases from the wall to the free stream. Because of this, a correct and accurate pressure gradient term is required to account for the convection term in momentum equation.

Emulsion on the other side can be described as a mixture of two liquids that would ordinarily not mix together. Two types of emulsion are temporary and permanent. An example of temporary emulsion is found in the industrial production of simple vinaigrette (mixture of oil and vinegar) and mixture of oil and water. When stirred or shaken vigorously, the two liquids tend to form temporary emulsion which comes together for a short time. In industry, Hollandaise sauce is another permanent emulsion which is made of egg yolks and clarified butter. These can be explained as good examples of a binary mixture of fluids. Fluid flow past a plate moving through a binary mixture has been investigated due to its importance in industry. Makinde et al. [11] carried out a research on unsteady convection with chemical reaction and radiative heat transfer past a flat porous plate moving through a binary mixture using the classical Boussinesq approximation. They assumed constant fluid viscosity within the thin boundary layer formed on vertical surface. The effects of increasing magnitude of thermal Grashof number, solutal Grashof number and other important parameters over velocity, temperature and concentration profiles were reported extensively. Makinde and Olanrewaju [12] went further to consider the flow of a viscous incompressible fluid flow past a vertical porous plate moving through a binary mixture with the influences of energy flux caused by a composition gradient and mass flux caused by a temperature gradient. They extensively reported the effect of the new parameters (i.e. Dufour and Soret parameter). Sastry and Murti [13] were motivated by the research and assumed that the fluid in question is electrically conducting and reported the effect of magnetic field parameter.

In view of these ideas, it is of importance to investigate the dynamics of fluids which contains microstructure as it flows past a vertical porous plate moving through a binary mixture as well (i.e. study fluid which contains particles that may undergo translations and rotations as it flows through a binary mixture). This kind of fluids belongs to a class of fluid with non-symmetric stress tensor that are called polar fluids. Physically, micropolar fluids consist of rigid, randomly oriented (or spherical) particles suspended in a viscous medium

where the deformation of fluid particles is ignored in Eringen [14,15] and also in [16]. Physical examples can be seen in ferrofluids, blood flows, bubbly liquids and liquids crystals [17,18]. In order to investigate such highly viscous fluid as it flows upward, Boussinesq approximation and temperature dependent viscosity are of great importance. Thermophoresis can be described as the migration of colloidal particle in response to a macroscopic temperature; when a temperature gradient is established in gas, small particles suspended in the gas migrate toward the direction of decreasing temperature. The phenomenon called thermophoresis occurs because gas molecules colliding on one side of a particle have different average velocities from those on the other side due to the temperature gradient. A common example of the phenomenon is the blackening of the glass globe of a kerosene lantern; the temperature gradient established between the flame and the globe drives the carbon particles produced in the combustion process toward the globe where they deposit [19]. Chamkha and Isaa [20] studied effects of heat generation/absorption and thermophoresis on hydromagnetic flow with heat and mass transfer over a flat surface. It is worth mentioning that in [19–21], the thermophoresis model is incorporated into the concentration equation and holds accurately when concentration at the wall is higher than that of the freestream. Recently, Animasaun [21] presented the effects of some thermo-physical parameters on non-darcian MHD dissipative Casson fluid flow along linearly stretching vertical surface with migration of colloidal particles in response to macroscopic temperature.

Natural convection flow occurs frequently in nature. It occurs due to positive temperature differences, as well as due to concentration differences or the combination of these two. For example in atmospheric flows, there exists differences in water concentration and hence the flow is influenced by such concentration difference. Convection in which the buoyancy forces are due to both temperature and chemical concentration gradients is referred to as thermo-solutal, or double diffusive convection. Changes in fluid density gradients may be caused by non-reversible chemical reaction in the system as well as by the differences in molecular weight between values of the reactants and the products. In the study of buoyancy driven flow, the model is built on the fact that average temperature of the fluid layers (T) is greater than the temperature of the fluid layers at free stream (T_∞). Boussinesq [22] studied buoyancy-driven flow; he studied density differences and acceleration due to gravity in relation to buoyancy driven flow [22]. The basis of the Boussinesq approximation is that there are fluid flows in which the temperature varies little and therefore the density varies little, yet the buoyancy drives the motion. Thus, the variation in density is neglected everywhere except in the buoyancy term.

Following the above contributions to the body of knowledge, a thorough literature review on Boussinesq approximation reveals that this model is valid accurately when both dimensional and dimensionless temperatures at the wall are higher in magnitude than the dimensional and dimensionless freestream temperatures; otherwise, thermal Grashof number may be negatively influenced. It is worth mentioning that this is dependent on the kind of similarity variable for temperature that is adopted. Likewise, when investigating fluid flow with temperature dependent dynamic viscosity and thermal conductivity, differences between wall and free stream temperature must be greater than zero. If otherwise, Grashof related parameter may be influenced badly. Typical effect on velocity profile when magnitude of thermal grashof number is unity has been presented in figures two and three of [11,12]. In both figures, it is observed that velocity profile reaches negative values few distance after the wall. Within past few years, modification of theory or model has been something researchers embrace and investigate in order to test the validity as presented in academic discourse. In order to demonstrate the effects of temperature dependent physical properties for natural convection in a concentric annulus, a modified Boussinesq approximation with temperature dependent viscosity and thermal conductivity was developed and used successfully in [23]. It is worth mentioning that the formulation was based on the primitive variables stated in [23]. Recently, Diaz et al. [24] reported that in the Boussinesq approximation the main coupling term is the buoyancy force (generation of momentum due to temperature gradients) together with viscous heating (heat production due to internal friction). It is always assumed that viscous heating is negligible. These researchers proposed a modification of the classical Boussinesq approximation for buoyancy-driven flows of viscous, incompressible fluids in situations where viscous heating cannot be neglected.

Motivated by the above investigations, the purpose of this research is to propose a modification of Boussinesq approximation and temperature dependent viscosity model which shall provide better analysis of highly viscous fluid as it flows along vertical surface when temperature at the wall is lesser than temperature at the free stream. The present paper studies the problem of unsteady convection with thermophoresis, chemical reaction and radiative heat transfer in a micropolar fluid as it flows past vertical porous plate moving through a binary mixture considering temperature dependent dynamic viscosity and constant vortex viscosity. This aim can be further described as an extension of [11–13] and modification of Boussinesq approximation together with temperature dependent viscosity. The governing equations are converted to couple ordinary differential equations by applying the similarity transformation. Numerical solutions of the reduced nonlinear similarity equations are then obtained by adopting numerical approach. The results of the numerical solution are then presented graphically as well as the skin friction, heat transfer, surface couple stress and mass transfer which are displayed in tabular forms for different values of parameters.

2. Basic equations

An unsteady micropolar fluid flow past a flat vertical porous surface moving through a binary mixture is considered. The flow is assumed to be in the x-direction which is taken along infinite surface and y-axis is normal to it. Since the plate is of infinite length in x-direction, therefore all the physical quantities (i.e. velocity, temperature, micro-element rotation and species concentration) except possibly the pressure are assumed to be independent of x. The fluid is assumed to be optically thin with absorption coefficient $\alpha \ll 1$. Following Cheng [25], the approximate form of the radiative heat flux equation $\frac{\partial q_r}{\partial y}$ is taken as the fourth power of temperature in the energy balance equation. In this research, it is assumed that there exist colloidal particles in the fluid which migrate due to the response of macroscopic temperature from the free stream T_∞. For boundary layer analysis, the temperature gradient along the surface is much lower than the temperature gradient normal to the surface, i. e.

$$\frac{\partial T}{\partial y} \gg \frac{\partial T}{\partial x} \tag{1}$$

In view of this, the component of thermophoretic velocity along the surface is negligible compared to the component of its velocity normal to the surface. Kabir and Al-Mahbub [26] reported that the effect of thermophoresis is usually prescribed by means of an average velocity that a particle will acquire when exposed to a temperature gradient. It is assumed that a very small amount of heat energy is transferred by convection into the boundary layer formed over a vertical flat surface at constant temperature T_w which is embedded in a fluid-saturated porous medium at constant ambient temperature T_∞ such that $T_w < T_\infty$. Considering the mathematical model introduced by [11] which is an extension of [12,13], Eringen [14,15], Ferdows et al. [27] together with all assumptions stated above along with Boussinesq's approximation, the governing equations can be formulated as follows:

The Continuity Equation

$$\frac{\partial v}{\partial y} = 0 \tag{2}$$

The Momentum Equation

$$\frac{\partial u}{\partial t} + v\frac{\partial u}{\partial y} = \left(\frac{\mu+\tau}{\rho}\right)\frac{\partial^2 u}{\partial y^2} + \frac{\tau}{\rho}\frac{\partial N}{\partial y} + g\beta(T-T_\infty) + g\beta^*(C-C_\infty) \tag{3}$$

The Angular Momentum Equation

$$\frac{\partial N}{\partial t} + v\frac{\partial N}{\partial y} = \frac{\gamma^*}{\rho j}\frac{\partial^2 N}{\partial y^2} - \frac{\tau}{\rho j}\left(2N + \frac{\partial u}{\partial y}\right) \tag{4}$$

The Energy Equation

$$\rho C_p\left(\frac{\partial T}{\partial t} + v\frac{\partial T}{\partial y}\right) = \kappa\frac{\partial^2 T}{\partial y^2} + Q - 4\sigma\alpha^2 T^4 \tag{5}$$

The Concentration Equation

$$\frac{\partial C}{\partial t} + v\frac{\partial C}{\partial y} + \frac{\partial}{\partial y}[V_T(C-C_\infty)] = D_m\frac{\partial^2 C}{\partial y^2} - R_A \tag{6}$$

As micropolar fluid flows along a vertical porous plate moving through a binary mixture of chemically reacting fluid, the usual quantities and constituents stated in Eqs. (5) and (6) are enough to justify the model. It is a well-known fact in the study of emulsion that the two liquids do not ordinary mix together; hence, most quantities/phenomena in a mixture theory are neglected. From Eq. (2), it can be noted that the velocity component (v) along y-direction is either constant or a function of time. Following Makinde [28], velocity component along y-axis is considered as

$$v = -c\sqrt{\frac{\vartheta}{t}} \tag{7}$$

where $c > 0$ is the suction parameter and $c < 0$ is the injection parameter. Spin gradient viscosity and Micro-inertia per unit mass are considered as stated in Abdel-Rahman [29] and Khan et al. [30] as

$$\gamma^* = \left(\mu + \frac{\tau}{2}\right)j, \qquad j = \frac{\mu}{\rho U_o} \tag{8}$$

In this study, $Q = (-\triangle H)R_A$ is the heat of chemical reaction called activation enthalpy and $R_A = K_r e^{-\frac{E_A}{R_G T}}C^n$ is the Arrhenius type of the nth order irreversible reaction, K_r is the chemical reaction rate, R_G is the universal gas constant and E_A is the activation energy parameter. The thermophoretic velocity of the colloidal particles in the fluid as incorporated in Eq. (6) was given by Talbot et al. [31] and later by Tsai et al. [32] as

$$V_T = -\frac{K^{th}}{T_{ref}}\left(\frac{\partial T}{\partial y}\right) \tag{9}$$

K^{th} is the thermophoretic coefficient which ranges in values from 0.2 to 1.2 as reported by Batchelor and Shen [33]. It is further assumed that all the fluid properties are constant except dynamic viscosity and the influence of density variation with temperature and concentration in the body force term (Boussinesq's approximation). According to Boussinesq [22], if ρ_∞ denotes the density of the fluid at the freestream where the temperature is T_∞ then for small temperature difference between the wall and freestream layer, the density model is presented as

$$\rho = \rho_\infty[1 - \beta(T - T_\infty)] \tag{10}$$

Buoyancy term $g(\rho - \rho_\infty)$ is of the same order of magnitude as the inertia term or the viscous term; so it is not negligible. Upon using the above approximation in Eq. (10), the buoyancy term can be simplified as

$$g(\rho - \rho_\infty) = -g\beta\rho_\infty(T - T_\infty) \tag{11}$$

The body force term (Buoyancy force) is now of the form $\rho g_x = g\beta\rho_\infty(T - T_\infty)$. For free convection, heat and mass transfer, the Boussinesq approximation is mathematically denoted in momentum equation as

$$\rho g_x = g\beta\rho_\infty(T - T_\infty) + g\beta^*\rho_\infty(C - C_\infty). \tag{12a}$$

Likewise, for forced convection, heat and mass transfer is mathematically denoted in momentum equation as

$$-\frac{\partial p}{\partial x} = u_e\frac{du_e}{dx} \tag{12b}$$

Also, for mixed convection, heat and mass transfer, the presure gradient term and Boussinesq approximation are mathematically denoted in momentum equation as

$$-\frac{\partial p}{\partial x} + \rho g_x = u_e\frac{du_e}{dx} + g\beta\rho_\infty(T - T_\infty) + g\beta^*\rho_\infty(C - C_\infty) \tag{12c}$$

This theory is known as Boussinesq approximation which states that density differences are sufficiently small to be neglected, except where they appear in terms multiplied by g (the acceleration due to gravity) see Boussinesq [22]. The essence of the Boussinesq approximation is that the difference in inertia is negligible but gravity is sufficiently strong to make the specific weight appreciably different between the two fluids. Through literature review, researchers have considered $0.1 \leqslant \theta_w \leqslant 1.5$. This can be further categorized into two cases which are: Case 1 when $\theta_w > 1$ (i. e. $\theta_w = 1.5$). Case 2 when $\theta_w < 1$ (i. e. $\theta_w = 0.1$). For more details on case 1 (see Animasaun [34]). In this research, $\theta_w < 1$ is only considered. When the fluid temperature $T(y,t)$ is subjected to $T(0,t) = T_w$ and $T(\infty,t) = T_\infty$ in which similarity variable for temperature as in [11–13] is considered, dimensionless wall temperature $\theta_w < 1$ simply implies $T_w < T_\infty$. In order to investigate the effect of temperature dependent viscosity, emphasis needs to be made on source of temperature into the fluid domain. Hence, it is necessary to modify Boussinesq's approximation in momentum equation and temperature dependent variable fluid viscosity model. It is very important to remark that if any model

as stated in Eq. (12a–c) is incorporated into the momentum equation when $T_w < T_\infty$, this may have negative influence on the boundary layer analysis. Typical negative influence can be deduced from Fig. 4 in [12]. To address this kind of negative influence which may not be suitable and accommodated when investigating fluid flow over a vertical/horizontal melting surface or vertical surface at absolute zero, a modified Boussinesq approximation is needed. In order to accurately achieve one of the objectives of this research (i.e. to investigate effects of temperature dependent variable fluid viscosity on free convective micropolar fluid flow past a vertical plate moving through a binary mixture considering a case when $[\theta_w, \phi_w] < 1$), the modified Boussinesq approximation is proposed as

$$\rho g_x = g\beta\rho_\infty(T_\infty - T) + g\beta^*\rho_\infty(C_\infty - C) \tag{13}$$

Based on the fact that typical examples of case 2 are common in the industry, correct governing equation(s) is/are needed. It is worth pointing out that it is valid, reliable and realistic to investigate case 2 mentioned above by substituting Eq. (13) into Eq. (3).

The temperature dependent viscosity model was developed using experimental data presented by Batchelor [35], adopted by Mukhopadhyay [36] and successfully used to analyze the effect of increasing temperature on viscosity within boundary layer in [37,38] as $\mu(T) = \mu^*[1 + b(T_w - T)]$ valid when $T_w > T_\infty$ is also modified to

$$\mu(T) = \mu^*[1 + b(T_\infty - T)] \tag{14}$$

It is worth mentioning that the new model as in (14) is valid when $T_w < T_\infty$. There are several temperature dependent shear viscosity models e.g. exponential model, Arrhenius model, Williams Landel–Ferry model, Masuko–Magill model and Batchelor model. All these models are developed for either liquid or gases in which vortex viscosity is zero. In this research, the author only considered a case where dynamic viscosity μ is temperature dependent and vortex viscosity τ is negligibly affected by temperature; hence it is assumed constant. It is worth mentioning that an experimental data which can unravel the influence of temperature on both dynamic and vortex viscosity as in the case of Micropolar fluid is still an open question. Since vortex viscosity is assumed as a constant, it is valid to assumed the new model in Eq. (14). Imposing the modified Boussinesq approximation (13) and temperature dependent variable fluid viscosity (14) on dimensional equations, Eqs. (3)–(6) becomes

$$\frac{\partial u}{\partial t} + v\frac{\partial u}{\partial y} = \frac{\mu(T)}{\rho}\frac{\partial^2 u}{\partial y^2} + \frac{1}{\rho}\frac{\partial u}{\partial y}\frac{\partial \mu(T)}{\partial T}\frac{\partial T}{\partial y} + \frac{\tau}{\rho}\left(\frac{\partial^2 u}{\partial y^2} + \frac{\partial N}{\partial y}\right) + g\beta(T_\infty - T) + g\beta^*(C_\infty - C) \tag{15}$$

$$\frac{\partial N}{\partial t} + v\frac{\partial N}{\partial y} = \left(\frac{\mu(T)}{\rho} + \frac{\tau}{2\rho}\right)\frac{\partial^2 N}{\partial y^2} - \frac{\tau U_o}{\mu(T)}\left(2N + \frac{\partial u}{\partial y}\right) \tag{16}$$

$$\rho C_p\left(\frac{\partial T}{\partial t} + v\frac{\partial T}{\partial y}\right) = \kappa\frac{\partial^2 T}{\partial y^2} + K_r e^{-\frac{E_A}{R_G T}} C^n(-\triangle H) - 4\sigma\alpha^2 T^4 \tag{17}$$

$$\frac{\partial C}{\partial t} + v\frac{\partial C}{\partial y} + (C_\infty - C)\frac{\partial V_T}{\partial y} + V_T\frac{\partial}{\partial y}(C_\infty - C) = D_m\frac{\partial^2 C}{\partial y^2} - K_r e^{-\frac{E_A}{R_G T}} C^n \tag{18}$$

The appropriate boundary conditions of the above problem are

$$u(y,0) = 0, \quad T(y,0) = T_w, \quad N(y,0) = -m_o\frac{\partial u}{\partial y},$$
$$C(y,0) = C_w \quad for \quad t \le 0 \tag{19}$$

$$u(0,t) = 0, \quad T(0,t) = T_w, \quad N(0,t) = -m_o\frac{\partial u}{\partial y},$$
$$C(y,t) = C_w \quad for \quad t > 0 \tag{20}$$

$$u(\infty,t) \to U_o, \quad T(\infty,t) \to T_\infty, \quad N(\infty,t) \to 0,$$
$$C(\infty,t) = C_\infty \quad for \quad t > 0 \tag{21}$$

In the boundary conditions Eqs. (19)–(21), $T_w < T_\infty$ and $C_w < C_\infty$. In Eq. (17) the case $m_o = 0$, is called strong concentrations by Guram and Smith [39] indicates $N(0,t) = 0$ near the wall, represents concentrated particle flows in which the microelements close to the wall surface are unable to rotate [40]. The case $m_o = 0.5$ indicates the vanishing of anti-symmetric part of the stress tensor and denotes weak concentrations [41]. The case $m_o = 1$, as suggested by Peddieson [42], is used for the modeling of turbulent boundary layer flows (see Ioan [16]). In this research, the case $m_o = 0.5$ is considered. Upon introducing the following dimensionless variables

$$f(\eta) = \frac{u}{U_o}, \quad \eta = \frac{y}{2\sqrt{\vartheta t}}, \quad \theta(\eta) = \frac{T}{T_\infty} \quad \theta_w = \frac{T_w}{T_\infty},$$
$$\phi(\eta) = \frac{C}{C_\infty}, \quad \phi_w = \frac{C_w}{C_\infty}, \quad N(\eta) = \frac{U_o}{\sqrt{\vartheta t}}h(\eta),$$
$$G_r = \frac{4tg\beta}{U_o b}, \quad G_c = \frac{4tg\beta^*}{U_o b}, \quad \aleph = \frac{\kappa}{\rho C_p}, \quad \xi = bT_\infty,$$
$$K_1 = \frac{\tau}{\mu}, \quad L_1 = K_1 U_o t, \quad \lambda = -\frac{K^{th}T_\infty}{\vartheta T_{ref}}$$
$$h_q = \frac{(-\triangle H)C_\infty}{\rho C_p T_\infty}, \quad R_a = \frac{4\sigma\alpha^2 T_\infty^4}{\rho C_p T_\infty}, \quad \omega = \frac{E_A}{T_\infty R_G},$$
$$D_a = 4tK_r e^{-\frac{E_A}{R_G T_\infty}} C^{n-1}, \quad P_r = \frac{\vartheta}{\aleph}, \quad S_c = \frac{\vartheta}{D_m} \tag{22}$$

into (15)–(21), the following dimensionless nonlinear ordinary differential equations are obtain

$$[1 + \xi - \theta\xi + K_1]\frac{d^2 f}{d\eta^2} - \xi\frac{d\theta}{d\eta}\frac{df}{d\eta} + 2(\eta + c)\frac{df}{d\eta} + 2k_1\frac{dh}{d\eta} + G_r\xi(1 - \theta) + G_c\xi(1 - \phi) = 0, \tag{23}$$

$$\frac{d^2\theta}{d\eta^2} + 2P_r(\eta + c)\frac{d\theta}{d\eta} + P_r h_q D_a e^{\omega\left(\frac{\theta-1}{\theta}\right)}\phi^n - P_r\theta^4 R_a = 0, \tag{24}$$

$$\left[1 + \xi - \theta\xi + \frac{K_1}{2}\right]\frac{d^2 h}{d\eta^2} + 2(\eta + c)\frac{dh}{d\eta} + 2h - \frac{L_1}{[1 + \xi - \theta\xi]}\left(8h + 2\frac{df}{d\eta}\right) = 0, \tag{25}$$

$$\frac{d^2\phi}{d\eta^2} + 2S_c(\eta + c)\frac{d\phi}{d\eta} - \lambda S_c(1 - \phi)\frac{d^2\theta}{d\eta^2} + \lambda S_c\frac{d\phi}{d\eta}\frac{d\theta}{d\eta} - S_c D_a e^{\omega\left(\frac{\theta-1}{\theta}\right)}\phi^n = 0 \tag{26}$$

The dimensionless boundary conditions of the above problem are

$$f(\eta)=0,\quad \theta(\eta)=\theta_w(<1),\quad h(\eta)=-\frac{1}{4}\frac{df}{d\eta},$$
$$\phi(\eta)=\phi_w(<1)\quad at\quad \eta=0 \tag{27}$$
$$f(\eta)\to 1,\quad \theta(\eta)\to 1,\quad h(\eta)\to 0,\quad \phi(\eta)=1$$
$$as\quad \eta\to\infty \tag{28}$$

where $f(\eta)$ is the dimensionless velocity function, ξ is the temperature dependent variable fluid viscosity parameter, K_1 is known as micro-rotation parameter, G_r is the modified thermal Grashof number, G_c is the modified solutal Grashof number, $\theta(\eta)$ is the dimensionless temperature function, P_r is the Prandtl number, h_q is the heat generation parameter, D_a is Damkhler number, ω is the activation energy parameter, R_a is the radiation parameter, $h(\eta)$ is the dimensionless micro-rotation function, L_1 is the time dependent micro-rotation parameter, $\phi(\eta)$ is the dimensionless concentration function, S_c is known as Schmidt number and λ is the thermophoretic parameter. Also, other quantities of physical interest in this problem are the skin friction C_f, Nusselt number N_u and Sherwood numbers S_h which are defined by Makinde et al. [11] as

$$C_f=\frac{2\vartheta\sqrt{t}}{U_o\sqrt{\vartheta}}\left(\frac{\partial u}{\partial y}\Big|_{y=0}\right)=\left(\frac{df}{d\eta}\Big|_{\eta=0}\right),\quad N_u=\frac{2\sqrt{\vartheta t}}{T_\infty}\left(\frac{\partial T}{\partial y}\Big|_{y=0}\right)=-\left(\frac{d\theta}{d\eta}\Big|_{\eta=0}\right)$$

$$S_h=\frac{2\sqrt{\vartheta t}}{C_\infty}\left(\frac{\partial C}{\partial y}\Big|_{y=0}\right)=-\left(\frac{d\phi}{d\eta}\Big|_{\eta=0}\right) \tag{29}$$

results of the skin friction, Nusselt number, and Sherwood number can be easily computed using Eq. (29).

3. Numerical solution

Numerical solutions of the ordinary differential Eqs. (23)–(26) with the Neumann boundary conditions (27) and (28) are obtained using classical Runge–Kutta method along with shooting technique. The set of coupled ordinary differential equations along with boundary conditions has been reduced to a system of eight simultaneous equations of first order for eight unknowns following the method of superposition (see Na [43]). In order to integrate the corresponding I.V.P. the values of $f'(0), \theta'(0), h'(0)$ and $\phi'(0)$ are required, but no such values exist after the non-dimensionalization of the boundary conditions (19) and (21). The suitable guess values for $f'(0)$, $\theta'(0)$, $h'(0)$ and $\phi'(0)$ are chosen and then integration is carried out. The calculated values for $f(\eta)$, $\theta(\eta), h(\eta)$ and $\phi(\eta)$ at $\eta_\infty=6$ are compared with the given boundary conditions in Eq. (28) and the estimated values $f'(0)$, $\theta'(0)$, $h'(0)$ and $\phi'(0)$ are adjusted to give a better approximation for the solution. For more details on the numerical technique see [44]. Series of values for $f'(0)$, $\theta'(0)$, $h'(0)$ and $\phi'(0)$ are considered and applied with fourth-order classical Runge–Kutta method using step size $\triangle\eta=0.01$. The above procedure is repeated until asymptotically converged results is obtained within a tolerance level of 10^{-5}. It is worth mentioning that there exist no related published articles that can be used to validate the accuracy of the numerical results. Eqs. (23)–(28) can easily be solved using ODE solvers such as MATLAB's `bvp4c` solver.

3.1. Verification of the results

In order to verify the accuracy of the present analysis, the results of Classical Runge–Kutta together with shooting have been compared with that of `bvp4c` solution for the limiting case when $\xi=3$, η at infinity $=6$, $G_r=G_c=1$, $D_a=0.05$, $\omega=R_a=0.2$, $K_1=\lambda=L_1=1$, $P_r=0.71$, $h=3$, $n=1$ and $\theta_w=\phi_w=0.1$ at various values of S_c and c. The comparison in the above cases is found to be in good agreement, as shown in Table 1. The excellent agreement is an encouragement for further study of the effects of other parameters on the flow.

4. Numerical results and discussion

Numerical computations have been carried out for the present problem by employing the similarity solution for $f(\eta)$, $\theta(\eta)$, $h(\eta)$ and $\phi(\eta)$ against η with variations of thermo-physical parameters controlling the fluid dynamics in the flow regime. The values of Schmidt number for hydrogen $S_c=0.22$ at 25 °C and one atmospheric pressure are considered in the analysis of the solution. It should be mentioned here that $D_a>0$ indicates an increase in the destructive chemical reaction rate, while $D_a<0$ corresponds to an increase in generative chemical reaction rate. The value of the Prandtl number is chosen to be $P_r=0.71$, which represents air at 25 °C and one atmospheric pressure. When modified local thermal Grashof number $G_r>0$ this corresponds to cooling of the surface and when $G_r<0$ this corresponds to heating of the surface. In addition, when modified local solutal Grashof number $G_c>0$ this indicates that the chemical species concentration in the free stream region is less than the concentration at the surface/wall and when $G_r<0$ this indicates that the chemical species concentration in the free stream region is greater than the concentration at the surface/wall. It is

Table 1 Comparison of local heat transfer rate $-\theta'(0)$ and local mass transfer rate $-\phi'(0)$ with S_c using Classical Runge–Kutta together with shooting techniques and `bvp4c` when $\eta_\infty=6$.

	$-\theta'(0)$RK4SM	$-\theta'(0)$ `bvp4c`	$-\phi'(0)$RK4SM	$-\phi'(0)$ `bvp4c`
$S_c=0.22,\ c=0$	−0.838686692972656	−0.838687	−0.582727235867182	−0.582727
$S_c=0.42,\ c=0$	−0.849242983648582	−0.849243	−0.860039307005880	−0.860039
$S_c=0.62,\ c=0$	−0.854912516033717	−0.854913	−1.099421579293592	−1.099422
$S_c=0.22,\ c=0.5$	−1.267068597902801	−1.267069	−0.798091264284715	−0.798091
$S_c=0.42,\ c=0.5$	−1.280521268663868	−1.280521	−1.279330713448670	−1.279331
$S_c=0.62,\ c=0.5$	−1.287403287660129	−1.287403	−1.728144872634346	−1.728145

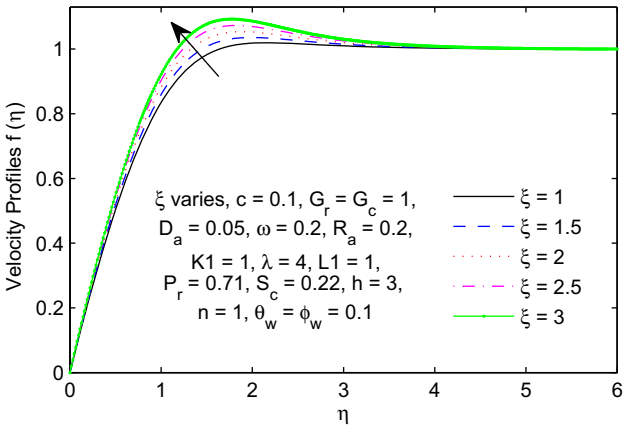

Figure 1 Velocity profiles for different values of ξ.

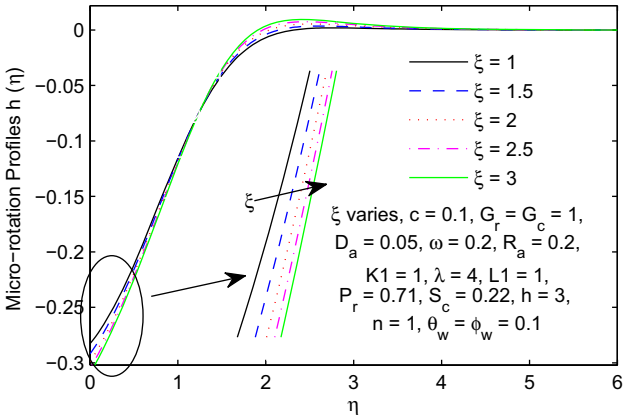

Figure 2 Micro-rotation profiles for different values of ξ.

observed from Table 1 that in the absence of suction (i. e. $c = 0$), both heat transfer rate and mass transfer rate decrease with an increase in Schmidt number. It is furthered seen that these physical quantities highly decrease with an increase in S_c.

At constant vortex viscosity, Fig. 1 illustrates the influence of the temperature dependent dynamic viscosity on the velocity distributions when modified local Grashof numbers $(G_r, G_c) = 1$, thermophoretic parameter $(\lambda = 4)$, micro-rotation parameter $(K_1 = 1)$ and time dependent micro-rotation parameter $(L_1 = 1)$. As magnitude of ξ increases, the velocity profiles asymptotically increase to its peak within $1.2 \leqslant \eta \leqslant 1.8$. Thereafter, each profile tends to satisfies the far field boundary condition asymptotically. As the micropolar fluid flows along the surface, it becomes heated about the wall in the process as magnitude of ξ increases. At a constant value of b, increase in ξ simply implies increase in the amount of input temperature from the free stream into the micropolar fluid domain. It is observed that velocity profiles near $4 \leqslant \eta \leqslant 6$ are not influenced with increase in ξ. The mathematical model of viscous forces by the differential equation assumes that the flow is moving along a parallel solid surface and the y-axis perpendicular to the flow. However, the relationship between shear stress and shear rate is nonlinear since non-Newtonian fluid is under consideration. Yet, any fluid moving along solid surface will incur a shear stress on that boundary and still obey no-slip condition. This accounts for the main reason why effect of ξ is very strong about the wall. From Engineering point of view, when the fluid heats up, its molecules become excited and begin to move (i. e. intermolecular force which holds all the fluid molecules so tight is weaken). The energy of this movement is enough to overcome the forces that bind the molecules together, allowing the fluid to move faster and decreasing its viscosity gradually away from the wall; hence, the velocity increases from the wall $(\eta = 0)$ to the free stream $(\eta = 3.8)$ with an increase in the value of ξ.

The influence of temperature dependent dynamic viscosity parameter (ξ) over micro-rotation distribution across the boundary layer is shown in Fig. 2. The result indicates that with increase in the parameter ξ, the micro-rotation of the particles in the fluid decreases very near the wall $(0 \leqslant \eta \leqslant 0.18)$, increases significantly within $(0.23 \leqslant \eta \leqslant 3.4)$ and negligibly increases as $\eta \to 6$. This result implies that when vortex viscosity is a constant function of temperature, the micro-rotation of particles near the wall decreases due to the fact that fluid near the vertical porous wall is more viscous. Hence, the particles within the micropolar fluid are able to rotate faster within the fluid domain $(0.23 \leqslant \eta \leqslant 3.4)$ where drag caused by the wall is reduced and heat energy is able to break down the intermolecular forces of the fluid within this interval of η. This result is valid since it has been observed in Fig. 1 that heat energy generated by increasing ξ and free stream are highly significant few distance away from the wall. See Table 2 for further report. It is noticed that skin friction coefficient increases while couple stress at the wall decreases which implies increase in drag near the wall and weak translations of particles; hence this accounts for a decrease in micro-rotation of particles near the wall. This effect may also be discussed as the corresponding influence of heat energy at the wall which is of small magnitude since $\theta_w = 0.1$ (see Table 3 for further report).

Fig. 3 represents the velocity profiles for different values of suction parameter (c). It is expected that increase in suction parameter should correspond to decrease in velocity field from the wall to the free stream in a case where dimensionless temperature $\theta_{(\eta=0)} > \theta_{(\eta\to\infty)}$ [19]. The effect of increasing suction parameter c is to remove the low-momentum fluid around the hot wall and delays both transition and separation

Table 2 Values of $f'(0)$ and $-h'(0)$ for various values of ξ when $c = 0.1$, $G_r = G_c = 1$, $D_a = 0.05$, $\omega = 0.2$, $R_a = 0.2$, $K_1 = 1$, $\lambda = 1$, $L_1 = 1$, $P_r = 0.71$, $S_c = 0.22$, $h = 3$, $n = 1$, $\theta_w = \phi_w = 0.1$ and $\eta_\infty = 6$.

	$f'(0)$	$-h'(0)$
$\xi = 1$	1.186167400354258	−0.103656480881624
$\xi = 2$	1.282625175735648	−0.138093051629340
$\xi = 3$	1.345231358872995	−0.159805656736284

Table 3 Values of $f'(0)$, $-\theta'(0)$ and $-\phi'(0)$ for various values of c when $\xi = 3$, $G_r = G_c = 1$, $D_a = 0.05$, $\omega = 0.2$, $R_a = 0.2$, $K_1 = 1$, $\lambda = 1$, $L_1 = 1$, $P_r = 0.71$, $S_c = 0.22$, $h = 3$, $n = 1$, $\theta_w = \phi_w = 0.1$ and $\eta_\infty = 6$.

	$f'(0)$	$-\theta'(0)$	$-\phi'(0)$
$c = 0$	1.335731028494380	−0.838686692972656	−0.582727235867182
$c = 0.5$	1.395937990067792	−1.230068597902801	−0.798091264284715
$c = 1$	1.486721604027753	−1.753901025239213	−1.038334565710785
$c = 1.5$	1.604063491727130	−2.281614874607798	−1.297065074287978
$c = 2$	1.743089163837045	−2.837580328041057	−1.569462995721548

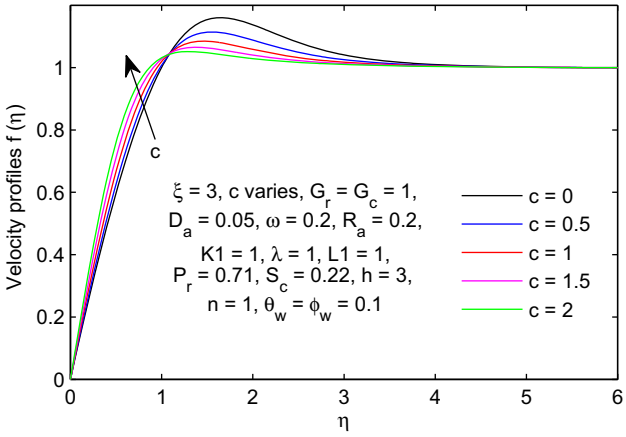

Figure 3 Velocity profiles for different values of c.

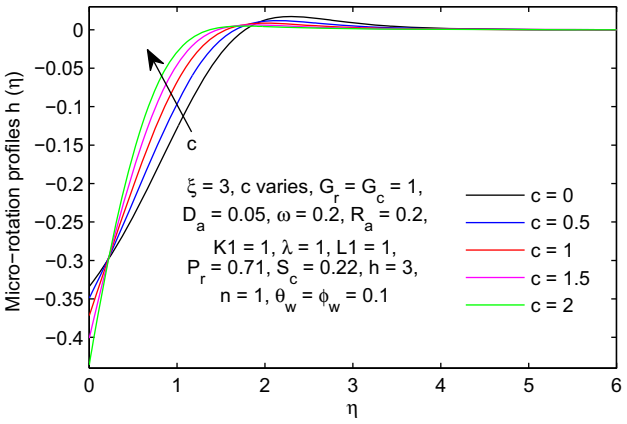

Figure 5 Micro-rotation profiles for different values of c.

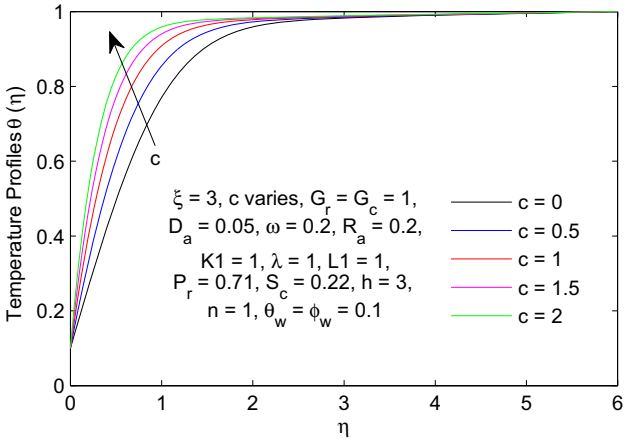

Figure 4 Temperature profiles for different values of c.

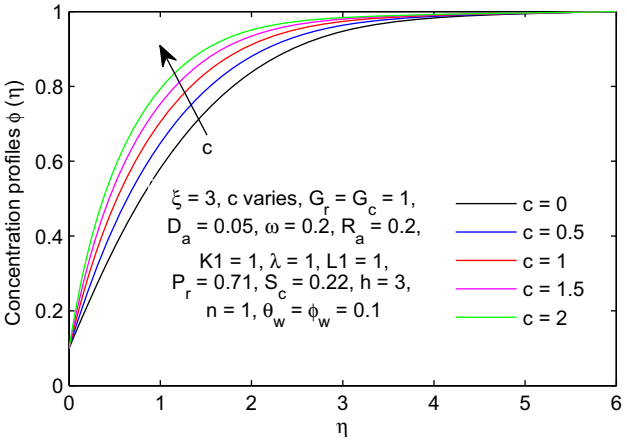

Figure 6 Concentration profiles for different values of c.

(i.e. stabilizes the boundary layer growth), since the fluid near the heated wall ($\eta = 0$) is pushed toward the wall where the buoyancy forces can act to retard the fluid due to high influence of the viscosity. The case is difference in this research, with an increase in suction ($c > 0$), it is observed that the velocity distributions increases near the vertical porous wall $0 \leqslant \eta \leqslant 1.1$ and decreases significantly thereafter. Low-momentum fluid around the hotter area due to $\xi = 3$ (within the fluid domain) and hottest fluid from freestream due to $\theta(\eta = 6) = 1$ are sucked. As the fluid is being sucked toward the wall, heat energy is also transferred toward the wall. This reduced the viscosity of the fluid and tends to increase the velocity. The negligible increase in the velocity near the wall can be further traced to the fact that the initial cold vertical wall before suction start was not in motion (U_o is the uniform velocity of the fluid layers at freestream) and dimensionless temperature $\theta_{(\eta=0)} < \theta_{(\eta=6)}$. The effect of suction parameter on the fluid temperature is highlighted in Fig. 4. It is observed that the fluid temperature increases near the wall and decreases negligibly far from the wall. As the flow develops along a vertical wall, one way of dealing with boundary layer transition (flow separation) is to suck the thin boundary layer through the vertical porous surface. As this method reduces drag, heat is escaped away from the flow regime; hence the temperature reduces as magnitude of suction increases. The variation of parameter c on the micro-rotation field is sketched in Fig. 5

Table 4 Values of $-\theta'(0)$ and $-\phi'(0)$ for various values of λ when $\xi = 3,\ G_r = G_c = 1,\ D_a = 0.05,\ \omega = 0.2,\ R_a = 0.2,\ K_1 = 1,\ c = 0.5,\ L_1 = 1,\ P_r = 0.71,\ S_c = 0.22,\ h = 3,\ n = 1,\ \theta_w = \phi_w = 0.1$ and $\eta_\infty = 6$.

	$-\theta'(0)$	$-\phi'(0)$
$\lambda = 1$	−1.267063097902801	−0.798091264284715
$\lambda = 2$	−1.271242106782623	−1.013393523684787
$\lambda = 3$	−1.274992930640617	−1.234174531599102

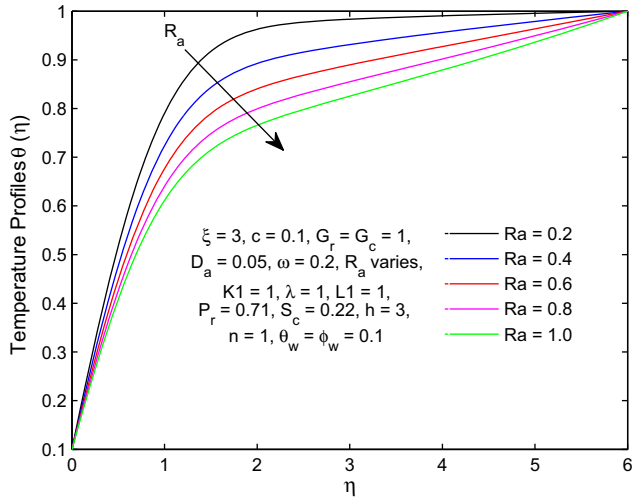

Figure 7 Temperature profiles for different values of R_a.

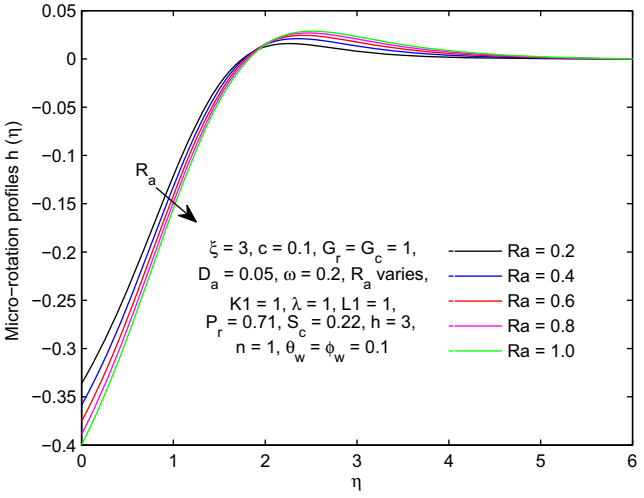

Figure 8 Micro-rotation profiles for different values of R_a.

when $\xi = 3$. It is found that $h(\eta)$ is a decreasing function of c near the wall $(0 \leqslant \eta < 0.25)$, increasing function thereafter $(0.27 < \eta \leqslant 1.9)$ and a positive decreasing function thereafter as $\eta \to 6$. The effect of suction parameter on the chemical species concentration in the boundary layer is depicted in Fig. 6 as the species migrates from the region of lower concentration $\phi(\eta = 0) = 0.1$ to region of higher concentration $\phi(\eta = 6) = 1$. From this figure, it is seen that the species concentration within the boundary layer increases with an increase in the magnitude of c. Numerical results for the heat transfer $-\theta'(0)$ and the mass transfer $-\phi'(0)$ as a function of thermophoretic velocity λ are shown in Table 4. It is observed from the table that both heat transfer and mass transfer decrease with an increase in the magnitude of λ.

The variations of temperature and micro-rotation profiles along with similarity variable with different values of radiation parameter are shown in Figs. 7 and 8. At a constant value of $\xi = 3,\ K_1 = 1$ and other parameters, it is seen that temperature of the fluid decreases with an increase in the magnitude of R_a. Physically, thermal radiation is found to be energy transfer by the emission of electromagnetic waves which carry energy away as the fluid flows along vertical surface moving through binary mixture. Since the increase in radiation parameter means increase in the rate at which heat energy is released from the flow region, this accounts for decrease in temperature distribution as the magnitude of parameter R_a increases. It is worth noticing that the significant decrease in temperature of the fluid within the domain greatly affects the micro-rotation as shown in Fig. 8. It is observed that, owing to the decrease in temperature profiles with an increase in R_a, the micro-rotation profiles decrease near the wall $(\theta_w = 0.1)$ and increase thereafter. Table 5 shows the effects of radiation parameter R_a on the heat transfer (temperature gradient) at the wall $(\eta = 0)$ and at the freestream $(\eta = 6)$. From the table, it is worth mentioning that the corresponding value of heat transfer is dependent on the value of Radiation parameter. Hence, the slope of the linear regression line S_{LR} through data points is estimated to explain the relationship. The S_{LR} through data points in $-\theta(\eta = 0)$ and R_a is estimated as 0.297158724731983. In addition, the S_{LR} through data points in $-\theta(\eta = 6)$ and R_a is esti-

Table 5 Values of $-\theta'(\eta = 0)$ and $-\theta'(\eta = 6)$ for various values of R_a when $\xi = 3,\ c = 0.1,\ G_r = G_c = 1,\ D_a = 0.05,\ \omega = 0.2,\ \lambda = 1,\ K_1 = 1,\ L_1 = 1,\ P_r = 0.71,\ S_c = 0.22,\ h = 3,\ n = 1,\ \theta_w = \phi_w = 0.1$ and $\eta_\infty = 6$.

	$-\theta'(\eta = 0)$	$-\theta'(\eta = 6)$
$R_a = 0.2$	−0.918684199255	−0.004155246447
$R_a = 0.4$	−0.828710139234	−0.020586841751
$R_a = 0.6$	−0.765065572559	−0.036772192146
$R_a = 0.8$	−0.716503253907	−0.052725901562
$R_a = 1$	−0.677628917187	−0.068460930666

mated as −0.080375214124880. Physically, the amount of heat energy at the wall is small and hence the temperature at this region is small. In view of this, the rate at which heat energy is transferred toward the wall increases with an increase in the magnitude of R_a. This accounts for the reason why $S_{LR} > 0$ and $S_{LR} < 0$ in the other case. As magnitude of R_a is increased from 0.2 to 1, the percentage increase of $-\theta(\eta = 0)$ is estimated as 26.23% while the percentage decrease of $-\theta(\eta = 6)$ is estimated as 1547.57%.

5. Conclusion

The present studies describes the boundary layer flow of unsteady convection with thermophoresis, chemical reaction and radiative heat transfer in a micropolar fluid flow past a porous vertical surface moving through a binary mixture. In a case of fluid flow along a vertical surface, the surface must be kept at temperature higher than that of the free stream in order to accurately utilize classical Boussinesq's approximation. If otherwise, modification of Boussinesq's approximation model and temperature dependent variable fluid viscosity model is necessary in order to accurately investigate the flow behavior. The governing partial differential equations are converted into ordinary differential equations by using similarity transformation before being solved numerically using the Runge–Kutta method along with shooting technique for $\eta \in [0, 6]$. The accuracy of the analysis is achieved by comparing the numerical solutions of Runge–Kutta with Shooting and `bvp4c`. Results for the skin friction coefficient, Nusselt number, velocity, temperature profiles as well as concentration profiles are presented for different values of the governing parameters. This study is able to acquaint us with the following facts and behavior of the fluid flow:

1. Velocity profile increases with an increasing temperature dependent variable fluid viscosity parameter. According to the obtained results, we conclude that velocity increases significantly near the wall where influence of heat energy generated by ξ and free stream are significant.
2. Due to temperature dependent variable fluid viscosity, the micro-rotation of particles decreases very close to the wall and increases significantly within the fluid domain where the effect of heat energy generated by both ξ and $\theta(\eta)$ at $\eta = 6$ can be greatly felt. Temperature of micropolar fluid as it flows along a surface moving through binary mixture is a decrease function of thermal radiation parameter.
3. The suction increases velocity near the wall where heat energy is low and decreases velocity close to free stream where heat energy is high. The effect of suction over velocity and micro-rotation of particles can be highly controlled by parameter ξ. Due to suction, both temperature and concentration inside the boundary layer increase.
4. Both heat transfer and mass transfer rates decrease with an increase in thermophoretic parameter. The imposition of Radiation heat transfer is to decrease the rate of heat transfer at freestream significantly.
5. The Modified Boussinesq Approximation will give better and correct analysis of fluid flow along vertical melting heat transfer surface. This recommendation is based on the fact that boundary conditions of temperature as in the case of melting heat transfer satisfy $T_m < T_\infty$.

Acknowledgments

The author wishes to express his sincere thanks to all the six anonymous Reviewers of this article for their valuable comments and suggestions. The Author also acknowledges the impact of Professor O.K. Koriko and Professor S.S. Motsa on his scientific research skills.

References

[1] Ezzat MA, Abd-Elaal MZ. Free convection effects on a viscoelastic boundary layer flow with one relaxation time through a porous medium. J Frank Inst 1997;334:685–706. http://dx.doi.org/10.1016/s0016-0032(96)00095-6.

[2] Ezzat MA, Othman MIA. Thermal instability in a rotating micropolar fluid layer subject to an electric field. Int J Eng Sci 2000;38:1851–67. http://dx.doi.org/10.1016/s0020-7225(00)00006-9.

[3] El-Hakiem MA. Natural convection in a micropolar fluid with thermal dispersion and internal heat generation. Int Commun Heat Mass Transfer 2004;31:117–1186. http://dx.doi.org/10.1016/j.icheatmasstranfer.2004.08.015.

[4] Ibrahim FS, Hassanien IA, Bakr AA. Unsteady magnetohydrodynamic micropolar fluid flow and heat transfer over a vertical porous plate through a porous medium in the presence of thermal and mass diffusion with a constant heat source. Can J Phys 2004;82:775–90. http://dx.doi.org/10.1139/P04-021.

[5] Ezzat M, El-Bary AA, Ezzat S. Combined heat and mass transfer for unsteady MHD flow of perfect conducting micropolar fluid with thermal relaxation. Energy Convers Manage 2011;52:934–45. http://dx.doi.org/10.1016/j.enconman.2010.08.021.

[6] Satya Narayana PV, Venkateswarlu B, Venkataramana S. Effects of Hall current and radiation absorption on MHD micropolar fluid in a rotating system. Ain Shams Eng J 2013;4:843–54. http://dx.doi.org/10.1016/j.asej.2013.02.002.

[7] Swapna G, Kumar L, Rana P, Singh B. Finite element modeling of a double-diffusive mixed convection flow of a chemically-reacting magneto-micropolar fluid with convective boundary condition. J Taiwan Inst Chem Eng 2015;47:18–27. http://dx.doi.org/10.1016/j.jtice.2014.10.005.

[8] Prakash D, Muthtamilselvan M. Effect of radiation on transient MHD flow of micropolar fluid between porous vertical channel with boundary conditions of the third kind. Ain Shams Eng J 2014;5:1277–86. http://dx.doi.org/10.1016/j.asej.2014.05.004.

[9] Gebhart B, Jaluria Y, Mahajan RL, Sammakia B. Buoyancy-induced flows and transport. New York: Hemisphere Publishing; 1988.

[10] Bird RB, Stewart WE, Lightfoot EN. Transport phenomena. New York: Wiley; 2007.

[11] Makinde OD, Olanrewaju PO, Charles WM. Unsteady convection with chemical reaction and radiative heat transfer past a flat porous plate moving through a binary mixture. Afrika Mat 2011;21:65–78. http://dx.doi.org/10.1007/s13370-011-0008-z.

[12] Makinde OD, Olanrewaju PO. Unsteady mixed convection with Soret and Dufour effects past a porous plate moving through a binary mixture of chemically reacting fluid. Chem Eng Commun 2011;198:920–38. http://dx.doi.org/10.1080/00986445.2011.545296.

[13] Sastry DRVSRK, Murti ASN. A double diffusive unsteady MHD convective flow past a flat porous plate moving through a binary mixture with suction or injection. J Fluids 2013. http://dx.doi.org/10.1155/2013/935156, 10 pages 935156.

[14] Eringen AC. Theory of micropolar fluids. J Math Anal Appl 1966;16:1–18.

[15] Eringen AC. Theory of thermomicrofluids. J Math Anal Appl 1972;38:480–96.

[16] Yacob N, Ishak A, Pop I. Melting heat transfer in boundary layer stagnation-point flow towards a stretching/shrinking sheet in a micropolar fluid. Comput Fluids 2011;47:16–21. http://dx.doi.org/10.1016/j.compfluid.2011.01.040.
[17] Lukaszewicz G. Micropolar fluids: theory and applications. Boston: Birkhauser; 1999.
[18] Reena, Rana US. Effect of dust particles on rotating micropolar fluid heated from below saturating a porous medium. Appl Appl Math 2009;4:189–217.
[19] Talbot L, Cheng RK, Scheffer RW, Wills DP. Thermophoresis of particles in a heated boundary layer. J Fluid Mech 1980;101:737–58.
[20] Chamkha AJ, Isaa C. Effects of heat generation/absorption and Thermophoresis on Hydromagnetic flow with heat and mass transfer over a flat surface. Int J Numer Methods Heat Fluid flow 2000;10:432–48. http://dx.doi.org/10.1108/09615530010327404.
[21] Animasaun IL. Effects of thermophoresis, variable viscosity and thermal conductivity on free convective heat and mass transfer of non-darcian MHD dissipative Casson fluid flow with suction and nth order of chemical reaction. J Nigerian Math Soc 2015;34:11–31. http://dx.doi.org/10.1016/j.jnnms.2014.10.008.
[22] Boussinesq J. Theorie de l'ecoulement tourbillonnant et tumultueux des liquides dans les lits rectilignes a grande section, Gauthier-Villars Paris vol. 1. Open Library OL7070543M; 1897.
[23] Shahraki F. Modeling of buoyancy-driven flow and heat transfer for air in a horizontal annulus: effects of vertical eccentricity and temperature-dependent properties. Numer Heat Transfer, Part A: Appl: Int J Comput Methodol 2002;42:603–21. http://dx.doi.org/10.1080/10407780290059729.
[24] Diaz JI, Rakotoson JM, Schmidt PG. A parabolic system involving a quadratic gradient term related to the Boussinesq approximation. Rev Real Acad Ciencias Ser A Matematicas (RACSAM) 2007;101:113–8.
[25] Cheng P. Two dimensional radiation gas flow by moment method. Am Inst Aeronaut Astronaut J 1964;2:1662–4.
[26] Kabir MdA, Al-Mahbub MdA. Effects of thermophoresis on unsteady MHD free convective heat and mass transfer along an inclined porous plate with heat generation in presence of magnetic field. Open J Fluid Dyn 2012;2:120–9. http://dx.doi.org/10.4236/ojfd.2012.24012.
[27] Ziaul Haque Md, Mahmud Alam Md, Ferdows M, Postelnicu A. Micropolar fluid behaviors on steady MHD free convection and mass transfer flow with constant heat and mass fluxes, joule heating and viscous dissipation. J King Saud Univ – Eng Sci 2012;24:71–84. http://dx.doi.org/10.1016/j.jksues.2011.02.003.
[28] Makinde OD. Free convection flow with thermal radiation and mass transfer past a moving vertical porous plate. Int Commun Heat Mass Transfer 2005;32:1411–9. http://dx.doi.org/10.1016/j.icheatmasstransfer.2005.07.005.
[29] Abdel-Rahman GM. Effect of magnetohydrodynamic on thin films of unsteady micropolar fluid through a porous medium. J Modern Phys 2011;2:1290–304. http://dx.doi.org/10.4236/jmp.2011.211160.
[30] Qasim M, Khan I, Shafie S. Heat transfer in a micropolar fluid over a stretching sheet with Newtonian heating. PLoS ONE 2013;8:e59393. http://dx.doi.org/10.1371/journal.pone.0059393.
[31] Talbot L, Cheng RK, Scheffer RW, Wills DP. Thermophoresis of particles in a heated boundary layer. J Fluid Mech 1980;101:737–58.
[32] Tsai R, Chang YP, Lin TY. Combined effects of thermophoresis and electrophoresis on particle deposition onto a Wafer. J Aerosol Sci 1998;29:811–25.
[33] Batchelor GK, Shen C. Thermophoretic deposition of particles in gas flowing over cold surfaces. J Colloid Interface Sci 1985;107:21–37, 195.
[34] Animasaun IL. Dynamics of unsteady MHD convective flow with thermophoresis of particles and variable thermo-physical properties past a vertical surface moving through binary mixture. Open J Fluid Dyn 2015;5:106–20.
[35] Batchelor GK. An introduction to fluid dynamics. Cambridge University Press; 1987.
[36] Mukhopadhyay S. Effects of radiation and variable fluid viscosity on flow and heat transfer along a symmetric wedge. J Appl Fluid Mech 2009;2:29–34.
[37] Animasaun IL, Anselm Oyem O. Effect of variable viscosity, dufour, soret and thermal conductivity on free convective heat and mass transfer of non-Darcian flow past porous flat surface. Am J Comput Math 2014;4:357–65. http://dx.doi.org/10.4236/ajcm.2014.44030.
[38] Aluko OB, Animasaun IL. Semi-analytic solution of non-linear coupled differential equation using adomian decomposition. World J Young Res 2013;3:23–30.
[39] Guram GS, Smith AC. Stagnation flows of micropolar fluids with strong and weak interactions. Comput Math Appl 1980;6:213–33.
[40] Jena SK, Mathur MN. Similarity solutions for laminar free convection flow of a thermo-micropolar fluid past a non-isothermal vertical flat plate. Int J Eng Sci 1981;19:1431–9.
[41] Ahmadi G. Self-similar solution of incompressible micropolar boundary layer flow over a semi-infinite plate. Int J Eng Sci 1976;14:639–46.
[42] Peddieson J. An application of the micropolar fluid model to the calculation of turbulent shear flow. Int J Eng Sci 1972;10:23–32.
[43] Na TY. Computational methods in engineering boundary value problems. New York: Academic Press; 1979.
[44] Dhanai R, Rana P, Kumar L. Multiple solutions of MHD boundary layer flow and heat transfer behavior of nanofluids induced by a power-law stretching/shrinking permeable sheet with viscous dissipation. Powder Technol; 2014 [in press]. doi:http://dx.doi.org/10.1016/j.powtec.2014.12.035.

Animasaun Isaac Lare was born and brought up in Osun State, Nigeria. He obtained his first degree (Bachelor of Technology in Pure and Applied Mathematics; Fluid Dynamics) from Ladoke Akintola University of Technology, Oyo State, Nigeria. He completed his second degree (Masters of Technology in Industrial Mathematics; Fluid Dynamics) at Federal University of Technology, Akure, Ondo State (FUTA). Presently, he is doing his third degree (Post Graduate Diploma in Education) in National Open University of Nigeria and also on his fourth degree (Doctor of Philosophy) in FUTA. His research interests are educational research (survey research), mathematical modeling, boundary layer analysis, heat and mass transfer, dynamics of Newtonian and non-Newtonian fluid, flow through porous or non-porous media, approximate and analytical solution of ordinary and partial differential equation.